Detection and Delimitation of Natural Gas in Seismic Images using MLP-Mixer and U-Net

Carolina L. S. Cipriano[1], Domingos A. D. Junior[1], Petterson S. Diniz[1], Luiz F. Marin[2],
Anselmo C. Paiva[1], João O. B. Diniz[1,3] and Aristófanes C. Silva[1]

[1]*Applied Computer Group NCA-UFMA, Federal University of Maranhao (UFMA), Sao Luís, Brazil*
[2]*Tecgraf Institute, Pontifical Catholic University of Rio de Janeiro (PUC-Rio), Rio de Janeiro, Brazil*
[3]*Fábrica de Inovação, Instituto Federal do Maranhão, Grajaú, Brazil*

Keywords: Hydrocarbons, Seismic Images, MLP-Mixer, U-Net, DenseNet, ResNet, Machine Learning.

Abstract: The seismic data acquired through the seismic reflection method is important for hydrocarbon prospecting. As an example of hydrocarbon, we have natural gas, one of the leading and most used energy sources in the current scenario. The techniques for analyzing these data are challenging for specialists. Due to the noisy nature of data acquisition, it is subject to errors and divergences between the specialists. The growth of deep learning has brought great highlights to tasks of segmentation, classification, and detection of objects in images from different areas. Consequently, the use of machine learning in seismic data has also grown. Therefore, this work proposes an automatic detection and delimitation of the natural gas region in seismic images (2D) using MLP-Mixer and U-Net. The proposed method obtained competitive results with an accuracy of 99.6% (inline) and 99.55% (crossline); specificity of 99.79% (inline) and 99.73% (crossline).

1 INTRODUCTION

Hydrocarbons are molecules made up of hydrogen and carbon. They are present in our energy resources, such as natural gas. The occurrence of hydrocarbons varies in space and time, as once important producing regions have already exhausted their reserves, and new ones are found in other areas (Teixeira et al., 2009).

Most analysis and prospecting rely on technology to detect and determine the extent of these deposits. Geophysical surveys in the gas industry are mainly conducted using seismic reflection techniques (Cox, 1999). Because they are more economical than good drilling, it is possible to extract data regarding the geometry and structure of the layers, rock types, lithology, and physical properties.

Due to the seismic data's low resolution and noisy nature, the data interpretation is challenging. The expert often creates several alternatives of the same seismic structure when in doubt. Furthermore, it is not uncommon for the team to disagree with the interpretation and consider that parts of the data can be reinterpreted (Patel et al., 2008). In this scenario, machine learning has been used for the segmentation,

classification, and detection of natural gas in 1D, 2D, and 3D seismic data.

In (Santos et al., 2019), they proposed a new approach to detect hydrocarbon indicators in seismic data using seismic trace and a Long Short-Term Memory (LSTM) neural network. They used a one-dimensional way along the seismic trace. In this process, each seismic trace was extracted using forty samples of window length of one sample overlapping each window. The public database used for gases identification was the Netherlands F3-Block. Using accuracy as the primary metric to automatically delimit gas pocket locations, the model achieved 97%.

In (El Zini et al., 2019) they proposed a bright spot detection method. Bright spots are strong indicators of the presence of natural gas. The model used SeisNet, a convolutional neural network with a "butterfly" architecture. The model also relied on data augmentation and transfer learning to overcome the data cap problem. The data used in SeisNet training is adopted from (Rizk et al., 2017) and consists of 110 grayscale images. As a result, it reached 95.6% of the F1 score and accuracy with an average absolute error that did not exceed 0.04% of the total volume.

Therefore, this work proposes an automatic detection method and delimitation of regions where natural gas accumulation can occur in 2D seismic images. It consists of MLP-Mixer for classifying these regions and U-Net for delimiting the extension of these accumulations.

As contributions of this research, we highlight 1) The use of the MLP-Mixer to detect the regions of interest, reducing the search field of these accumulations, and 2) An automatic 2D method of direct detection of hydrocarbons.

This paper is organized as follows: Section 2 presents the proposed method for automatic detection and delimitation of natural gas. Section 3 presents and discusses the results. Finally, Section 4 presents the final considerations of this study.

2 MATERIALS AND METHOD

This section details the steps of the proposed method. After data acquisition and processing, the proposed method consists of three main steps: 1) Model entry, where data preparation takes place; 2) Detection of the region of interest, where the classification of patches between gas and non-gas occurs; and 3) Gas delimitation, where the segmentation of the gas extension in the regions of interest occurs. Figure 1 summarizes these steps. And finally, the results are evaluated.

2.1 Data Acquisition

For this work, we used the public database called Netherlands F3-Block. F3 is a block in the Dutch sector of the North Sea covered by 3D seismic that was acquired to explore gas (Nubis, 1987). The F3 has gas markings for both inlines and crosslines (Tecgraf Institute (PUC-Rio)). Crosslines are perpendicular lines (Schlumberger, 2021a), while inlines are in the same direction of the data acquisition (Schlumberger, 2021b). The 3D seismic cube was delimited, as in (Santos et al., 2019) by Tecgraf Institute (PUC-Rio). And finally, converted to 2D as shown in Figure 2.

A seismic line within a 3D survey parallels the direction in which the data was acquired. In marine seismic data, the inline is one in the recording vessel that tows the coils.

2.2 Model Input

After acquiring and processing the 3D data into the 2D data, the slices were loaded and saved in grayscale

by the matplotlib python library, as shown in Figure 3. Due to the small amount of data (242 crossline slices and 449 inline slices) and the inline and crossline lines having different dimensions, we extracted 2D patches with a size of 128×128 to increase the number of samples and standardize these dimensions.

2.3 Gas Region Detection

After extracting patches at the model input, the samples were presented to the MLP-Mixer (Tolstikhin et al., 2021) for classifying gas patches and non-gas patches.

MLP-Mixer is a classification network with architecture based only on multilayer perceptrons. It's a competitive alternative that doesn't use convolutions or self-attention. And its architecture is based entirely on multilayer perceptrons (MLPs) that are repeatedly applied to spatial locations or resource channels. (Tolstikhin et al., 2021).

Figure 4 presents the MLP-Mixer architecture, where: input consists of patches extracted from the input image; mixer layer blocks and sorting head (Tolstikhin et al., 2021).
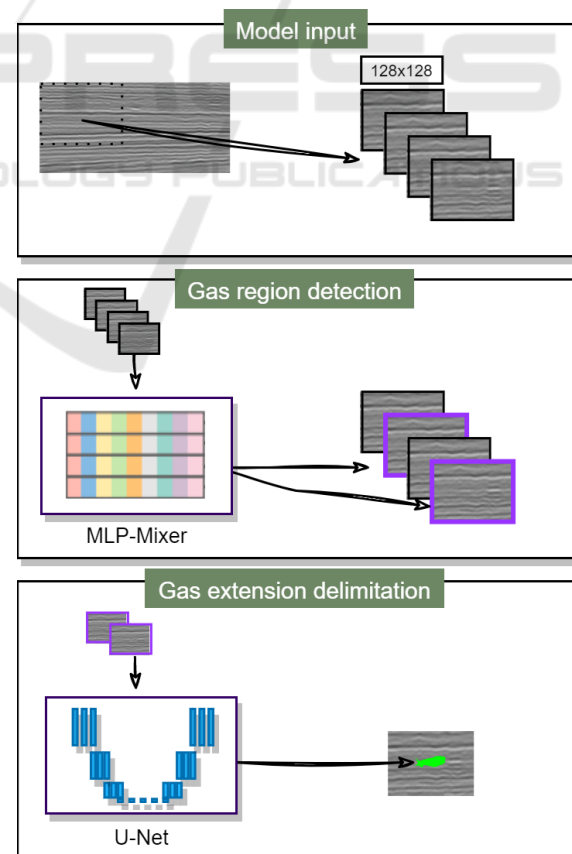
Figure 1: Steps of the proposed method.
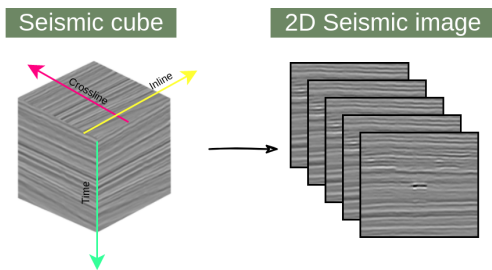
Figure 2: Illustrative picture. Seismic cube and 2D slices.
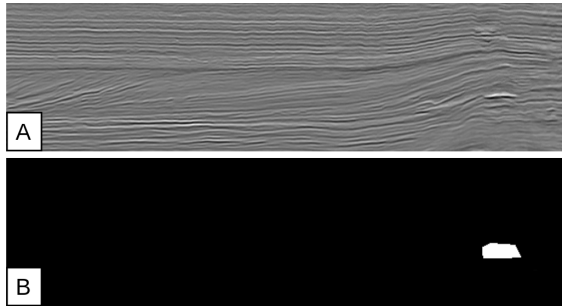
Figure 3: A) grayscale seismic image and B) corresponding binary marking (Tecgraf Institute (PUC-Rio)).
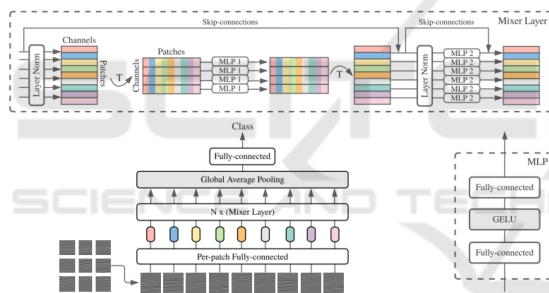
Figure 4: Adapted from MLP-Mixer architecture (Tolstikhin et al., 2021).

The input maintains the dimensionality of patches, which reduces the computational cost. The mixer layer block has two MLP layers, each consisting of two fully connected layers and a GELU nonlinearity: channel-mixing MLPs and token-mixing MLPs. Channel-mixing layer allows communication between different channels. Token-mixing layer allows communication between different spatial locations (tokens) (Tolstikhin et al., 2021). The head classifier contains dropout, Global average pooling, and softmax for classification.

2.4 Gas Extension Delimitation

After detecting gas regions by the classification networks, the samples classified as gas samples are presented to the Convolutional Neural Network (U-Net) for segmentation of the gas in the patches.

The U-Net was specially designed to segment medical images, but as it shows good results in other fields, it was chosen to delimit the gas extension. It is a fast network, relies heavily on data augmentation, and can be trained end-to-end from very few images (Ronneberger et al., 2015). U-Net simply concatenates the encoder feature maps to decoder feature maps at every step. This architecture allows the decoder to learn the relevant features lost when grouped in the encoder. Its concatenation connections at each step do this. Figure 5 introduces the U-Net architecture.
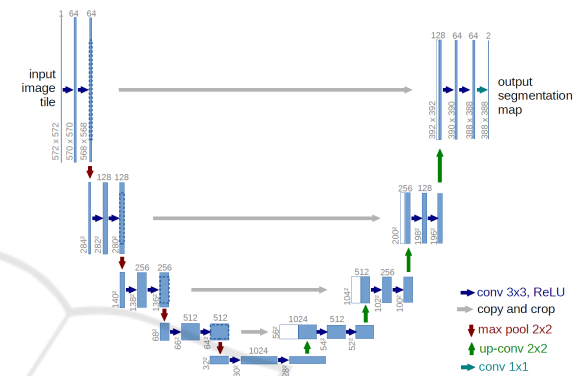
Figure 5: U-Net architecture (Ronneberger et al., 2015).

2.5 Validation

We used seven metrics commonly found in classification and segmentation problems to evaluate the results: Accuracy (ACC), Precision (PRE), Sensitivity (SEN), F1 score (F1), Specificity (SPEC), AUC, and Dice . These metrics evaluate the intersection between the real (expert marking) and what is proposed by the method (method result), as shown in the following equations:

$$Accuracy = \frac{TP+TN}{TP+FP+FN+TN} \qquad (1)$$

$$Precision = \frac{TP}{TP+FP} \qquad (2)$$

$$Sensitivity = \frac{TP}{TP+FN} \qquad (3)$$

$$F1-score = 2 * \frac{Precision * Sensitivity}{Precision + Sensitivity} \qquad (4)$$

$$Specificity = \frac{TN}{TN+FP} \qquad (5)$$

$$AUC = \frac{2TP}{2TP+FP+FN} \qquad (6)$$

$$Dice = \frac{2TP}{2TP + FP + FN} \tag{7}$$

Metrics are evaluated against image pixels. Where:

- The True Positive (TP) is the number of pixels classified as gas-containing pixels by the method and the expert.

- The False Negative (FN) is the number of pixels classified as pixels that do not contain gas by the method but were classified as pixels that contain gas by the expert.

- The False Positive (FP) is the number of pixels classified as pixels that contain gas by the method but were classified as pixels that do not contain gas by the expert.

- The True Negative (TN) is the number of pixels classified as gas-free pixels by the method and also by the expert.

3 RESULTS

This section presents and discusses the results achieved by the method developed for gas detection and delimitation in seismic images. The analysis sequence consists of 1) Training and testing, 2) Model Input, 3) Gas region detection and 4) Gas extension delimitation.

3.1 Training and Testing

The implementation was developed in Python 3.7 programming language, with Keras and TensorFlow frameworks for U-Net and MLP-Mixer. We used the Numpy package to manipulate the seismic data, and the OpenCV and Matplotlib libraries to manipulate the images. The machine used features hardware consisting of an Intel(R) Core(TM) i7-6700 CPU @ 3.40GHz, 16GB of RAM, and a 6GB GeForce GTX 1060 GPU.

3.2 Model Input

The public database called the F3 dataset (Section 2.1) contains 242 crossline and 449 inline lines. The crossline lines were randomly divided into 162 for training, 40 for validation, and 40 for testing. Likewise, the inline lines were divided into 329 for training, 60 for validation, and 60 for testing. We maintain the proportions according to (Santos et al., 2019) for comparative purposes..

To input the gas region detection models, 128x128 patches were extracted with an overlap of 10, as they showed better results in the MLP-Mixer than the results without overlap. Table 1 presents the number of samples generated for training, validation, and testing in the crossline and inline lines.

Table 1: Number of samples generated for gas region detection models.

	Files	Gas	No Gas	Total
Crossline				
Training	162	4133	16279	20412
Validation	40	1057	3983	5040
Test	40	64	336	400
Inline				
Training	329	10112	51082	61194
Validation	60	1809	9351	11160
Test	60	164	796	960

For the input of the gas extension delimitation model, we extract patches with 128x128 pixels without overlappingg, as they did not show significant improvements for U-Net. The number of samples generated for training, validation, and testing in the crossline and inline lines are presented in Table 2.

Table 2: Number of samples generated for the gas extension delimitation models.

	Files	Gas	No Gas	Total
Crossline				
Training	162	263	1357	1620
Validation	40	68	332	400
Test	40	64	336	400
Inline				
Training	329	876	4388	5264
Validation	60	152	808	960
Test	60	164	796	960

3.3 Gas Region Detection

In the gas region detection step, two models were generated: one for the inline lines and another for the crossline lines, according to the division in the Table 1. MLP-Mixer is a supervised classification architecture. Thus, for training the models (crossline and inline), the extracted patches were labeled as patches that contained gas and patches that did not contain gas.

For this work, we used the MLP-Mixer implementation of (Benjamin-Etheredge, 2021) for two classes. It has a patch size of 8 (The patch size must be divisible by the input data size); 4 mixer layer blocks; 64 MLP token dimension; MLP channel

dimension of 128; and, hidden dimension of 128, as shown in Table 3.

Table 3: Settings used in MLP-Mixer.

Input	128x128x1
Patch size	8
MLP token dimension	64
MLP channel dimension	128
Hidden dimension	32

The training configuration was defined for 25 epochs, using sparse categorical cross-entropy as a loss function and f1 score as a metric. The Table 4 presents the results for gas region detection in seismic images.

Table 4: Result of the gas region detection step.

	MLP-Mixer	
	Crossline	Inline
ACC (%)	96.15	98.55
SEN(%)	87.61	95.24
SPEC(%)	98.27	99.2
AUC (%)	92.94	97.22
PREC(%)	92.61	95.87
F1 (%)	90.04	95.56

For comparative purposes, other models were also used for the same delimitation task they were: ResNet (He et al., 2015) and the DenseNet (Huang et al., 2017). ResNet and DenseNet were used to extract features, then a classification block was added to both networks, as shown in Table 5.

Table 5: Classification block for the gas region detection comparison models.

Dense	512 + Relu
Dropout	0.5
Dense	256 + Relu
Dense	2 + Softmax

Table 6 presents results for gas region detection in seismic images with comparison models. As we can see, the MLP-Mixer achieved the best gas detection results compared to the ResNet and DenseNet models. Except for sensitivity and AUC in the crossline, DenseNet obtained a higher result.

In addition to the results, the MLP-Mixer presented a significantly superior performance concerning the training time, as shown in Table 7. This performance is because the MLP-mixer does not increase depth (channel) along with the layers, as with convolutional networks.

The MLP-Mixer proved to be an excellent classifier for seismic images despite not using

Table 6: Comparison of methods for gas detection.

	MLP-Mixer	ResNet	DenseNet
Crossline			
ACC (%)	96.15	90.6	95.54
SEN(%)	87.61	59.94	88.91
SPEC(%)	98.27	98.19	97.18
AUC (%)	92.94	79.07	93.04
PREC(%)	92.61	89.15	88.65
F1 (%)	90.04	71.68	88.78
Inline			
ACC (%)	98.55	98	97.03
SEN(%)	95.24	94.15	88.35
SPEC(%)	99.2	98.76	98.74
AUC (%)	97.22	96.45	93.54
PREC(%)	95.87	93.69	93.19
F1 (%)	95.56	93.92	90.71

Table 7: Comparison of models in relation to training time.

	Time (min)	
	Crossline	Inline
MLP-Mixer	33	101
ResNet	529	1308
DenseNet	837	2421

convolution and attention mechanisms as the main models currently. It obtained competitive results in a much shorter processing time.

3.4 Gas Extension Delimitation

In the delimitation step, we generated two models, one for the inline lines and another for the crossline lines. As U-Net is a semantic segmentation network, we extracted 128x128 patches from the respective gas and non-gas binary masks for training the models.

After some initial experiments with different parameters, we set the U-Net training configuration to 50 epochs with a batch size of 4, the Adam optimization function with a learning rate of 0.00001, decay of 0.000001, clipvalue = 0.5, and Dice as a loss and metric function validation evaluation.

Table 8 presents the final result of the proposed method. This result is the combination of the detection step and the delimitation step. The inline line method presents superior results to the crossline method in the detection and delimitation step. The reason is the outstanding amount of training images for the inline.

Table 9 presents a comparison of the results in relation to the work of (Santos et al., 2019). Improvements in accuracy were observed with 99.6% (inline) and 99.55% (crossline); specificity 99.79%(inline), and 99.74%(crossline), showing that

Table 8: Final result of the proposed method.

Base	F1 (%)	ACC (%)	PREC (%)	SEN (%)	SPEC (%)	AUC (%)	Dice (%)
Inline	84.18	99.6	84.0	86.85	99.79	93.32	84.18
Crossline	80.3	99.55	80.49	82.74	99.73	91.23	80.3

the proposed model was able to reduce the number of false positives. However, he could not overcome the sensitivity.

Table 9: Comparison of the proposed method with another work in the literature.

	Proposed	(Santos et al.,2019)
Crossline		
F1 (%)	80.3	-
ACC (%)	99.55	96.83
PREC(%)	80.49	-
SEN(%)	82.74	94.77
SPEC(%)	99.73	96.87
AUC (%)	91.23	98.71
Dice (%)	80.3	-
Inline		
F1 (%)	84.18	-
ACC (%)	99.6	97.16
PREC(%)	84.0	-
SEN(%)	86.85	97.83
SPEC(%)	99.79	97.15
AUC (%)	93.32	98.8
Dice (%)	84.18	-

Figure 6 presents a case that shows the contribution of MLP-Mixer in reducing false positives. As we can see in the picture 6 - C), U-Net mistakes the prediction of gas in regions similar to the region of interest.
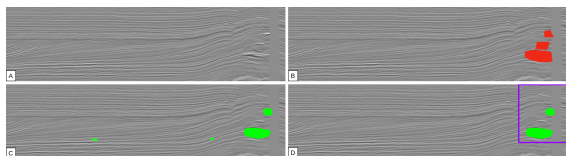
Figure 6: Crossline 909: A) Input image, B) Specialist marking, C) Gas extension delimitation isolated prediction result, D) Proposed model. The expert mark (red), gas region detection result (purple) and gas range delimitation result (green).

The approach of (Santos et al., 2019) of working with seismic trace (1D) has the advance of generating more data samples. Due to data imbalance, accuracy alone cannot reflect the method's performance. The precision shows that the proposed model could reduce the number of false positives, and the sensitivity indicates that the delimitation made by the U-Net suffered from the number of gas samples.

Next, we will see some examples of the results of the proposed method. The figure 7 shows the result where the MLP-Mixer was able to detect the gas region. And the U-Net precisely segments the gas.
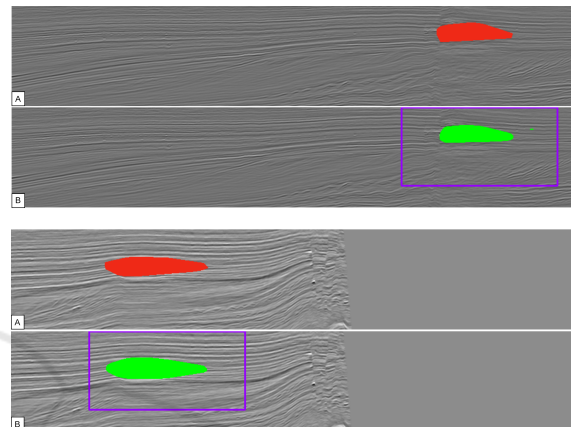
Figure 7: Inline 86 and 597: A) specialist marking; B) Prediction result for the proposed method. Result of gas region detection (purple) and result of gas extension delimitation (green).

Figure 8 also presents a good result from the MLP-Mixer, but with the difference that there are false negatives in the U-Net prediction.
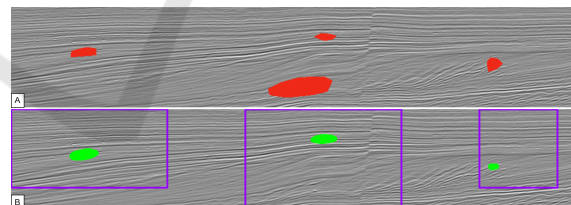
Figure 8: Inline 221: A) specialist marking; B) Prediction result for the proposed method. Result of gas region detection (purple) and result of gas extension delimitation (green).

Figure 9 presents a result where the MLP-Mixer was able to detect the gas region. And the U-Net precisely segments the gas.

Figure 8 also presents a good result from the MLP-Mixer, but with the difference that there are false negatives in the U-Net prediction.
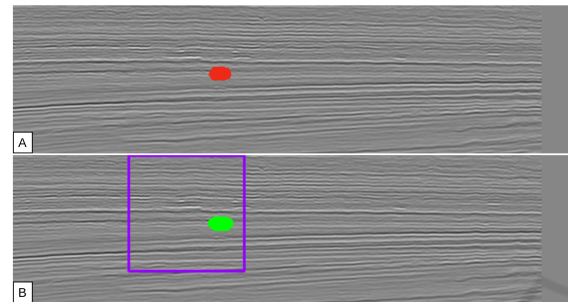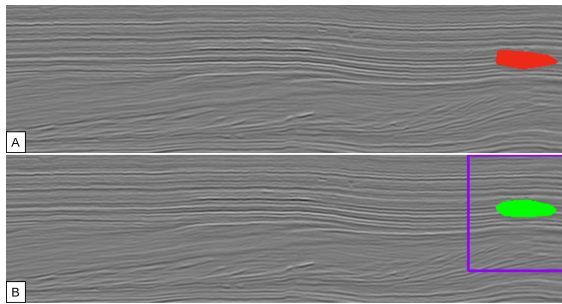
Figure 9: Crossline 511 and 100: A) specialist marking; B) Prediction result for the proposed method. Result of gas region detection (purple) and result of gas extension delimitation (green).
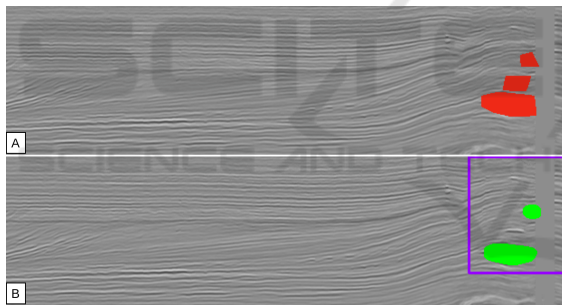
Figure 10: Crossline 909: A) specialist marking; B) Prediction result for the proposed method. Result of gas region detection (purple) and result of gas extension delimitation (green).

4 CONCLUSIONS

Due to its characteristics and the limited availability of public data, the automatic detection and delimitation of natural gas in seismic images is a difficult task. Gas occurrences have different locations and sizes, in addition to having a lot of noise that is derived from the acquisition process. These characteristics make the detection and delimitation process challenging since this location is difficult, even with the naked eye by the specialist.

The MLP-Mixer was very important to the method in the gas detection regions. It managed to perform well in the classification of regions and, consequently, contributed to the delimitation of gas only in the correct regions. The delimitation is a more difficult task, but even so, U-Net managed to have a relevant performance considering the imbalance of the gas and non-gas areas.

In general, the results for detection and delimitation of regions and gas were promising, achieving advances in accuracy with 99.6% (inline) and 99.55% (crossline); specificity 99.79% (inline) and 99.74% (crossline), compared to related work.

As future work, we identified the need to: 1) Use transfer learning techniques, since seismic data are scarce, deep learning models are sensitive to the amount of data and data increase had little contribution in experimental tests; 2) Use other semantic segmentation techniques for gas delimitation available in the literature; 3) And, finally, the use of seismic bases from other regions to test the generalization of the proposed model.

ACKNOWLEDGEMENTS

REFERENCES

Benjamin-Etheredge (2021). mlp-mixer-keras. https://github.com/Benjamin-Etheredge/mlp-mixer-keras0.

Cox, M. (1999). *Static corrections for seismic reflection surveys*. Society of Exploration Geophysicists.

El Zini, J., Rizk, Y., and Awad, M. (2019). A deep transfer learning framework for seismic data analysis: A case study on bright spot detection. *IEEE Transactions on Geoscience and Remote Sensing*.

He, K., Zhang, X., Ren, S., and Sun, J. (2015). Deep residual learning for image recognition. *CoRR*, abs/1512.03385.

Huang, G., Liu, Z., Van Der Maaten, L., and Weinberger, K. Q. (2017). Densely connected convolutional networks. In *Proceedings of the IEEE conference on computer vision and pattern recognition*, pages 4700–4708.

Nubis, T. (1987). Project f3 demo 2020.

Patel, D., Giertsen, C., Thurmond, J., Gjelberg, J., and Grøller, E. (2008). The seismic analyzer: Interpreting and illustrating 2d seismic data. *IEEE Transactions on*

Visualization and Computer Graphics, 14(6):1571–1578.

Rizk, Y., Partamian, H., and Awad, M. (2017). Toward real-time seismic feature analysis for bright spot detection: a distributed approach. *IEEE Journal of Selected Topics in Applied Earth Observations and Remote Sensing*, 11(1):322–331.

Ronneberger, O., Fischer, P., and Brox, T. (2015). U-net: Convolutional networks for biomedical image segmentation. In *International Conference on Medical image computing and computer-assisted intervention*, pages 234–241. Springer.

Santos, L. F., Silva, R. M. G. E., Gattass, M., and Silva, A. C. (2019). Direct hydrocarbon indicators based on long short-term memory neural network. In *SEG Technical Program Expanded Abstracts 2019*, pages 2373–2377. Society of Exploration Geophysicists.

Schlumberger (2021a). Oilfield glossary.

Schlumberger (2021b). Oilfield glossary.

Teixeira, W., Fairchild, T. R., Toledo, M. C. M. d., and Taioli, F. (2009). Decifrando a terra.

Tolstikhin, I., Houlsby, N., Kolesnikov, A., Beyer, L., Zhai, X., Unterthiner, T., Yung, J., Steiner, A., Keysers, D., Uszkoreit, J., et al. (2021). Mlp-mixer: An all-mlp architecture for vision. *arXiv preprint arXiv:2105.01601*.